Since January 2020 Elsevier has created a COVID-19 resource centre with free information in English and Mandarin on the novel coronavirus COVID-19. The COVID-19 resource centre is hosted on Elsevier Connect, the company's public news and information website.

Talanta 252 (2023) 123835

Contents lists available at ScienceDirect

Talanta

journal homepage: www.elsevier.com/locate/talanta

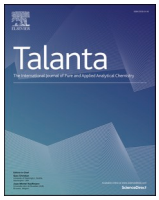

Multiple ligation–Assisted recombinase polymerase amplification for highly sensitive and selective colorimetric detection of SARS-CoV-2

Tasnima Alam Asa [a], Pradeep Kumar [a], Jaehyeon Lee [b], Young Jun Seo [a,*]

[a] Department of Chemistry, Jeonbuk National University, Jeonju, 54896, South Korea
[b] Department of Laboratory Medicine, Jeonbuk National University Medical School and Hospital, Jeonju, 54896, South Korea

ARTICLE INFO

Keywords:
Pyrophosphate
Colorimetric sensing
PK-probe
Isothermal amplification
Recombinase polymerase amplification (RPA)
SARS-CoV-2

ABSTRACT

In this paper we present a new method for the detection of severe acute respiratory syndrome coronavirus 2 (SARS-CoV-2), targeting a specific region "N gene." Under isothermal reaction conditions, we integrated ligation (Lig; high selectivity) and recombinase polymerase amplification (RPA; high sensitivity) processes, obtaining a robust method of detection. For point-of-care testing, we incorporated our laboratory-produced pyrophosphate ion (PPi)–sensing probe (**PK-probe**) for colorimetric analysis of the reaction. The total detection system was efficient and effective at diagnosing this RNA virus–mediated disease rapidly (30 min). In a full-genome SARS-CoV-2 study, our **PK-probe**/Lig-RPA system functioned with a limit of detection of 1160 copies/ml, with a single-mismatch level of selectively, and it was highly selective even in the presence of bacterial genomes commonly found in the human mouth and nose. This robust, straightforward, selective, efficient, and ultra-sensitive colorimetric detection method, with potential for point-of-care analysis, should also be effective in detecting a diverse range of other RNA-based diseases.

1. Introduction

The coronavirus disease 2019 (COVID-19) pandemic had a sudden devastating effect on global public health, taking more than 5.9 million lives alongside 445 million cases, while also collapsing the worldwide economy [1]. Maintaining regular diagnosis is important to prevent inadvertent infectious viral shedding and spreading in our communities, including asymptomatic infected persons and elders with disease comorbidities [2,3]. Despite the availability of many detection systems, including those based on microfluidic analytic, serological [4,5] and nucleic acid detection, there is room to develop efficient and effective systems for the diagnosis of COVID-19 and, thereby, control this crisis [6].

Specific and precise viral nucleic acid detection using the reverse transcription polymerase chain reaction (RT-PCR) has dominated serological testing; it has become the gold standard testing method, despite having limitations in, for example, sample storage, temperature control during incubation, expense, the need for purification and long analysis times, and false negative results arising from viral evolution, making it unsuitable for use at the point-of-care (POC) level [4,5]. Furthermore, RT-PCR and qPCR require standard/advanced PCR machines with trained personnel, so they are not suitable for POCT [2]. Considering the role of fomites in spreading infection, POC testing (POCT) is a high priority for diagnosis because it minimizes the need for complicated clinical practices and helps to accelerate decision-making in regard to optimized treatment. POCT should be simple, easy to perform, robust, portable, and require only small amounts of samples; it could, for example, employ constant-temperature isothermal detection of nucleic acids through the strand displacement activity of DNA polymerase [e.g., recombinase polymerase amplification (RPA), RCA, and LAMP] [6].

Many detection systems are well established, including those based on RT-RPA, RT-PCR, RT-LAMP, RT-RPA/CRISPR Cas12b, and qPCR [7–14]. In this present study we developed a system based on a pyrophosphate-sensing probe (**PK-probe**) and ligation–RPA (Lig-RPA) for the POCT. Although RT-RPA is quite simple and does not require an expensive equipment [15], there is significant drawback in the selectivity with the chance of mis- or self-pairing of the primers during the reverse transcription (RT) when targeting the whole genome of viral RNA; primers may not discriminate the exact target sequence from the non-target sequences with a few mismatches. RT-RPA system may produce many unwanted cDNA products during the reverse transcription [16]; some of the primers might bind nonspecifically to unwanted

* Corresponding author.
E-mail address: yseo@jbnu.ac.kr (Y.J. Seo).

https://doi.org/10.1016/j.talanta.2022.123835
Received 7 May 2022; Received in revised form 29 July 2022; Accepted 7 August 2022
Available online 14 August 2022

targets and produce nonspecific amplified products. Therefore, when designing the target sequence and primer, it is very difficult and requires careful design to obtain accurate results. Another problem is that it is difficult to apply the PK probe that can sense the pyrophosphate developed by our research team for POCT because unwanted pyrophosphate ion (PPi) will be released during the reverse transcription and, ultimately, leading false positive signals when applying our PPi-sensing PK Probe [17,18].

In our present proposed detection system based on **PK-probe**/Lig-RPA, the drawbacks of RT-RPA can be overcome while providing more accurate analysis [14]. In our system, the use of multiple Lig processes removes many of the complexities of the RT step (e.g., it avoids the possibility of mispairing of primers with different non-target sequences; no extra pyrophosphate is released during the ligation process; and high temperatures are avoided because the Lig and RPA reactions are both operated with incubation at room temperature) [15,16]. Thus, the whole process of **PK-probe**/Lig-RPA detection can be performed isothermally, simplifying the detection and making it suitable for POCT [17]. To avoid the side effects of the RT reaction, we selected the SplintR ligation reaction because it is robust and does not release any PPi, it produces the target gene (only 220-mers), and there is no chance of producing any other nonspecific amplified products during the RPA process (because of the availability of the "N gene," which is approximately a 220-mer) [18]. Thus, only the selected target can be amplified, such that the change in color produced by the **PK-probe** providing a more authentic outcome. The SplintR ligase–based ligation system is robust and approximately 100 times faster than the system based on T4 DNA ligase, thereby accelerating detection systems based on selective RNA-based DNA ligation [16]. The RT-RPA system is well established for highly sensitive and robust detection [8]. Nevertheless, selectivity has always remained problematic [19]. Gratifyingly, our present detection strategy, integrating rapid SplintR ligase–based ligation with RPA, operates with enhanced selectivity and high sensitivity when compared with other known detection systems [20–22].

Colorimetric detection is the fastest means of detection because it allows instant qualitative outcomes to be determined by the naked eye; it is, therefore, simple and suitable for POCT [23]. PPi is one of the most significant biological anions, performing various biophysiological functions, including many associated with the regulation of metabolism. In DNA/RNA synthesis, the most common byproduct is PPi, which acts as a pivotal indicator sensor of diagnostics [24,25]. Based on the concept of sensing PPi, we have developed a colorimetric probe (**PK-probe**) that senses PPi with sufficient selectivity over other types of anions, as well as DTT and cysteine [26]. Here we combined this **PK-probe** with the Lig-RPA reaction for the diagnosis of SARS-CoV-2, particularly targeting the "N gene" region. Our resulting **PK-probe**/Lig-RPA colorimetric isothermal nucleic acid detection system appears suitable for POCT because the process is simple and operates with high selectivity and sensitivity (Scheme 1) [27].

2. Experimental section

2.1. General information

All DNA oligonucleotides were purchased from Bioneer. SplintR ligase and the Isothermal Amplification Buffer Pack were obtained from New England Biolabs (USA). The RPA TwistAmp® Basic Kit was purchased from TwistDx, TABAS03KIT (USA). Formamide (F7503-100 ML) was purchased from Sigma–Aldrich (USA). UV–Vis absorption spectra were recorded using a Cary Series UV–Vis spectrophotometer (Agilent Technologies, USA). All optical measurements were performed at room temperature, using a quartz cuvette (path length: 1 cm). The **PK-probe** was prepared according to a previously reported procedure; its spectra were in accordance with those described [26].

Polyacrylamide gel electrophoresis (PAGE) was performed in 20% polyacrylamide gel. 40% Acrylamide/Bis solution (BIO-RAD, USA; 2.5 mL), 10X Tris borate EDTA buffer (Enzynomics, South Korea; 0.5 mL), and 20% ammonium persulfate (in H_2O) were mixed in a tube and distilled water then added to give a total volume of 5 mL. Finally, tetramethylethylenediamine (TEMED; Sigma–Aldrich, USA) was added to give the 20% polyacrylamide gel. The gels were loaded in an electrophoresis instrument (Mini-PROTEAN Tetra Cell; BIO-RAD, USA) and treated at 80 V for 6 h. The gels were stained with ethidium bromide (EtBr) solution for 10 min; the stained gels were washed with water for 10 min. Photographs of the gel and colorimetric detection images were captured using a mobile device under a transilluminator.

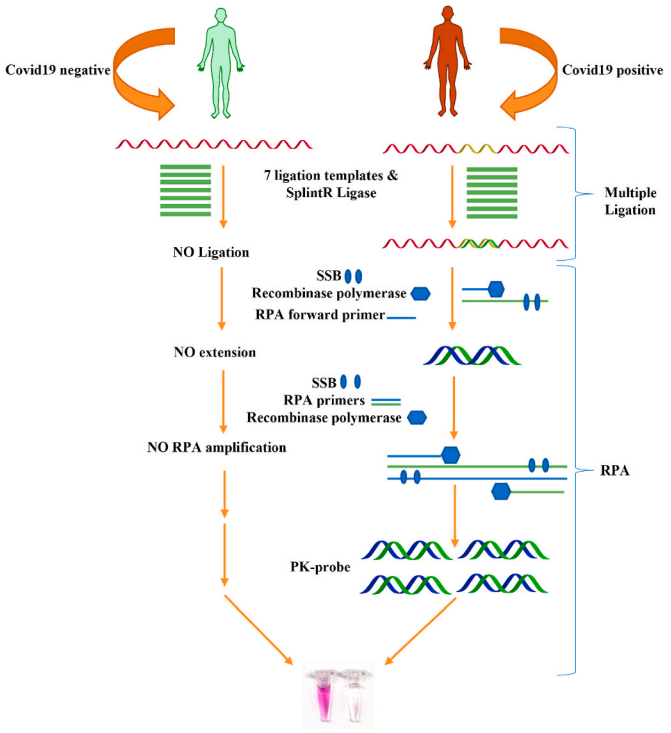

Scheme 1. Schematic representation of the **PK-probe**/Lig-RPA assay.

2.2. Ligation and RPA reaction conditions

The total ligation reaction volume was 10 μL, including the solution of the seven ligation oligonucleotide templates (10 nM, 5 μL), spiked SARS-CoV-2 RNA (2 copies; 1 μL) 10X SplintR ligase buffer (500 mM Tris-HCl, 100 mM $MgCl_2$, 10 mM ATP; pH 7.5 at 25 °C; 1 μL), 10X bovine serum albumin (BSA; 1 μL), SplintR ligase (25 U/μL; 1 μL), **PK-probe** (0.1 μL) and added dH_2O to give a total 10 μl volume and incubated at 37 °C for approximately 10 min.

Following the general procedure of the Twist Dx RPA kit, the total reaction volume of 50 μL contained the primer-free rehydration buffer (29.5 μL), forward and reverse primers (each 50 pmol/μL; 5 μL), 100 mM DTT (3 μL), and ligated target product (10 μL); it was treated with the Basic reaction kit mixture containing lyophilized enzymes, then mixed using a pipette. 280 mM $Mg(OAc)_2$ (2.5 μL) was added and mixed well. The reaction mixture was incubated at 37 °C for approximately 20 min.

2.3. Sensitivity and selectivity measurements

During preparation of SARS-CoV-2 spike RNA we made a simulated sample; a 200 μL (1000 copies) of recombinant SARS-CoV-2 full-genome control material (assigned as 5000 copies/mL; AccuPlex SARS-CoV-2 Molecular Controls Kit – Full Genome, Material Number 0505–0129, SeraCare, Milford, MA) -was spiked into 1.8 mL buffer (eNAT, Copan Italia, Brescia, Italy) of negative human sample prepared according to standard specimen acquisition. Then this total 2 ml solution (1000

copies) were extracted using an eMAG system (bioMerieux, MarcylEtoile, France), following the extraction protocol provided by the manufacturer, with an input volume of 200 μL (100 copies) and obtained an elution volume of 50 μL (100 copies). The copy concentration in the extracted RNA was approximately 2 copies/μL = 2000 copies/ml.

For the sensitivity study, the RNA sample was diluted in distilled water and lyophilized to give concentrations varying from 0 to 50 copies/μL = 0 to 50,000 copies/ml. All the samples at each concentration were tested with the **PK-probe**/Lig-RPA system; the absorbances were measured to calculate the limit of detection (LOD). The selectivity study involved nine species of bacteria that are known normal flora in the upper respiratory tract (*Staphylococcus aureus*, *Staphylococcus epidermidis*, *Enterococcus faecalis*, *Enterococcus feacium*, *Escherichia coli*, *Klebsiella pneumoniae*, *Enterobacter cloacae*, *Pseudomonas aeruginosa*, and *Acinetobacter baumannii*). All of the bacterial DNA was extracted using the boiling method, with DNA extraction buffer (Seegene, Seoul, South Korea); viral RNA was extracted in the same manner of validation with clinical samples. The extracted bacterial DNA and viral RNA were tested with the **PK-probe**/Lig-RPA system; their results were compared with those for SARS-CoV-2 detection. In the sensitivity and selectivity studies, water (150 μL) was added into a 250-μL reaction tube along with 25 mM **PK-probe** (0.1 μL) to check for a color change and later diluted with dH2O to make a 1 mL solution for detailed analysis, because the absorbance of each reaction mixture was measured in the presence of **PK-probe**.

3. Results and discussion

3.1. Selection of target site and primer design

Based on our hypothesis, we designed seven templates (Lig T1, Lig T2, Lig T3, Lig T4, Lig T4, Lig T5, Lig T6, Lig T7) for the synthesis of cDNA (targeting the "N gene" of SARS-CoV-2) mediated by SplintR ligase (Table S1). Among them, the LT2 to LT7 templates presented a monophosphate unit at the 5′-end for the ligation event. The templates containing a phosphate modification at the 5′-end would also allow the ligation by SplintR ligase to occur in the presence of perfectly matched target RNA; during the ligation reaction no PPi would be released as a byproduct. In the presence of the RNA target ligation would occur without any chance of PPi being released, unlike the situation during RT. We designed two primers (Lig-RPA fwd pri, Lig-RPA rev pri) for the RPA amplification process. To examine the selectivity, we designed some mismatched templates (Lig-T3 tail 1 mm, Lig-T4 mid 1 mm, Lig-T4 2 mm) with one and two base-mismatches; the mismatched points are highlighted in red in Table S1. We prepared a 220bp-long cDNA targeting "N gene" in SARS-CoV-2 by ligation of seven templates (ca. 32bp each) and then examined the RPA reaction. Designing the templates for binding to the specific region of viral RNA for the ligation reaction was the significant step for selective detection; it would form the full-length cDNA only when each template had bound to the target "N gene" in SARS-CoV-2. For this study we used 100 copies of spike SARS-CoV-2 full-genome RNA and attempted to clarify the cDNA formation using the seven templates and SplintR ligase; we analyzed the outcome through PAGE (Fig. 1(A)). We confirmed the formation of the 220mer cDNA

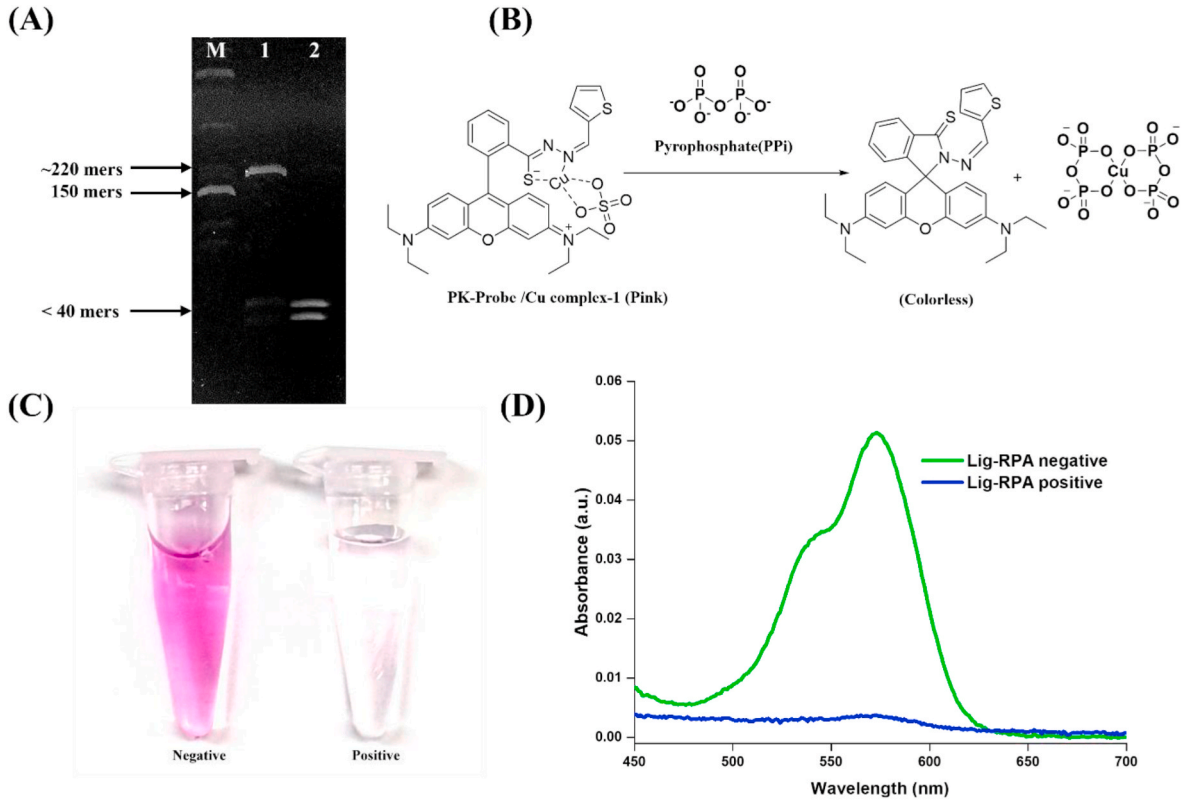

Fig. 1. Demonstration of the **PK-probe**/Lig-RPA assay. **(A)** Confirmation of the Lig-RPA reaction, using PAGE; lane M: 25/100 bp ladder; lane 1: extracted whole-genome RNA from SARS-CoV-2–positive patient + 1 to 7 ligation templates corresponding to the "N" gene of SARS-CoV-2 + ligation and RPA reaction mixture with **PK-probe**; lane 2: extracted whole-genome RNA from SARS-CoV-2–negative patient + 1 to 7 ligation templates corresponding to the "N" gene of SARS CoV-2 + ligation and RPA reaction mixture with **PK-probe**. Near the <40mer size location, some bands are visible for both lane 1 (blurry, very light) and lane 2 (clear), representing unreacted ligation templates and RPA primers that were approximately 30–36 mers in length (Table S1). **(B)** Color change mechanism of **PK-probe** [26]. **(C)** Optimization of **PK-probe**/Lig-RPA; a concentration of **PK-probe** of 2.5 μM was required to optimize the visibly significant color change between the positive and negative reactions. **(D)** Absorbances of negative and positive **PK-probe**/Lig-RPA assays. All absorbances were measured at 575 nm. (For interpretation of the references to color in this figure legend, the reader is referred to the Web version of this article.)

indirectly after RPA. We observed a specific band at approximately the 220mer location when we added the "N gene" in SARS-CoV-2 (lane 1); in the absence of the target, we did not observe any corresponding band, implying that no ligation had occurred (lane 2). Thus, the PAGE data confirmed that our Lig-RPA system was working.

3.2. PK-probe combined with Lig-RPA system

PK-probe is a Cu^{2+} complex of a thienyl-hydrazone rhodamine derivative. Several Cu^{2+}-complex probes have been used in the colorimetric detection of DNA/RNA amplification [28]; even though they were selective to PPi, they underwent cross reactions with DTT [29]. Another type of AuNCs-Cu^{2+} system has been used to detect PPi in human urine [30]. Nevertheless, **PK-probe** is the probe that has exhibited high selectivity toward PPi in the presence of natural deoxynucleotide triphosphates (dNTPs), DTT, and cysteine. **PK-probe** is a pink-colored probe featuring a ring-opened rhodamine entity complexed to a Cu^{2+} ion. When this probe comes in contact with PPi, that ion forms a complex with Cu^{2+} ion previously coordinated to the rhodamine entity. After **PK-probe** releases its Cu^{2+} ion, self-driven rhodamine ring closure occurs, resulting in disappearance of the pink color [Fig. 1(B)]. Even though DTT is a good competitor for forming Cu^{2+} complexes, **PK-probe** releases its Cu^{2+} ion selectively to PPi, resulting in a large decrease in absorbance at 575 nm in the presence of PPi. This selective and specific colorimetric sensor for PPi is highly resistant to all other biomolecules and buffer components, particularly large amounts of DTT and human serum.

Based on the working mechanism of **PK-probe**, we tested whether we could detect SARS-CoV-2 using a combination of **PK-probe** and the Lig-RPA system.

To examine the utility of the **PK-probe**/Lig-RPA system, we tested negative conditions (in the absence of the target "N gene" in SARS-CoV-2) and positive conditions (in presence of target "N gene" in SARS-CoV-2) and examined their responses at various **PK-probe** concentrations. A concentration of 2.5 μM was optimal for our Lig-RPA system. Fig. 1(C) reveals that a significant color change between the positive and negative reactions was visible to the naked eye. In Fig. 1(D), according to the absorbance readings based on the qualitative control, there was also drastic difference measured at a wavelength of 575 nm.

3.3. Optimization diagnostic process for POCT

During optimization of the **PK-probe**/Lig-RPA detection assay, we checked the activity of our system based on temperature and time. In the time-dependent study, we tested the combination of **PK-probe**/Lig-RPA from 0 min to 1 h; it had already been proven that 10 min would be sufficient for ligation by SplintR ligase, with that RPA would take less than 20 min to amplify even one copy number of DNA [16,31]. The **PK-probe**/Lig-RPA system already provided a significant differentiable colorimetric outcome to the naked eye within a total diagnosis time of 20 min (Lig, 10 min; RPA, 10 min); after 50 min, almost clear visibility had occurred (Fig. 2A and B). Thus, we believed that the **PK-probe**/-Lig-RPA system could detect the target "N gene" in SARS-CoV-2 within 30 min with a visible color change.

Next, we optimized the temperature for the POCT. SplintR ligase is reported to display its optimized activity at 37 °C, while for RPA the optimized activity is reported to occur at 39–42 °C; nevertheless, enzymes can be activated at temperatures as low as 16 °C, and both enzymes can function well even at room temperature [10,16,32]. If detection is possible under ambient conditions/room temperature, then POCT would be simpler and more feasible to perform; therefore, we tested our Lig-RPA assay at various temperatures, including 20, 25, 30,

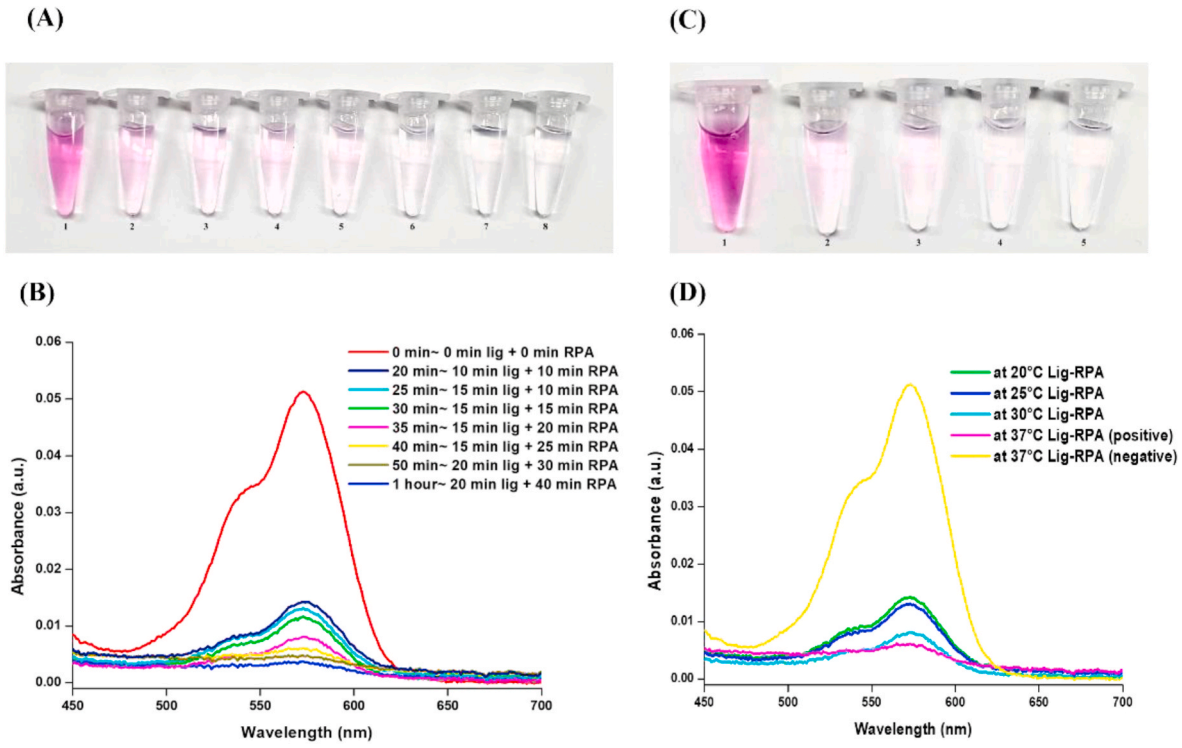

Fig. 2. Optimization of **PK-probe**/Lig-RPA assay. **(A)** Colorimetric analysis of time-dependent sensitivity. Lane 1: 0 min – 0 min Lig + 0 min RPA; lane 2: 20 min – 10 min Lig + 10 min RPA; lane 3: 25 min – 10 min Lig + 15 min RPA; lane 4: 30 min – 15 min Lig + 15 min RPA; lane 5: 35 min – 15 min Lig + 20 min RPA; lane 6: 40 min – 15 min Lig + 25 min RPA; lane 7: 50 min – 20 min Lig + 30 min RPA; lane 8: 1 h – 20 min Lig + 40 min RPA. **(B)** Absorbance spectra according to the colorimetric tests in (A). **(C)** Colorimetric analysis of temperature dependent study. Lane 1: at 37 °C Lig-RPA (negative); lane 2: at 20 °C Lig-RPA; lane 3: at 25 °C Lig-RPA; lane 4: at 30 °C Lig-RPA; lane 5: at 37 °C Lig-RPA (positive). **(D)** Absorbance spectra of the **PK-probe**/Lig-RPA system according to the temperature-dependent study in (C). All absorbances were measured at 575 nm.

and 37 °C (Fig. 2C and D). We found that our system is worked well in the range 20–37 °C; even at 20 °C the outcome of the assay was satisfactory for qualitative analysis, although the efficiency was higher at 37 °C.

3.4. Sensitivity

We examined the sensitivity of detection when using our **PK-probe**/Lig-RPA system. To ensure similar conditions for calculation of the LOD we made a simulated sample; we used spiked SARS-CoV-2–positive RNA sample with an assigned copy number (2 copies/μl), and prepared samples of various concentrations for the sensitivity study. We measured the sensitivity in terms of the absorbance at 575 nm. We performed the sensitivity tests using from 0 to 50 copies/μl = 0 to 50,000 copies/ml; their reactions were confirmed using PAGE [Fig. 3(A); corresponding colorimetric data in Fig. 3(B)].

From Fig. 3(A), PAGE analysis of the sensitivity experiments using different copy numbers revealed a specific amplified product (ca. 220mer) when using 1 to 50 copy numbers of target SARS-CoV-2 RNA, whereas the 0 copy case resulted in no band visibility at this position. A colorimetric study (Fig. 3(B)) revealed that the 0-copy reaction provided a whole pink color, whereas increasing the target copy number resulted in more colorless properties of the **PK-probe**. We performed this experiment three times to determine the sensitivity, based on the absorbance at 575 nm (Fig. S1). We measured the average change in absorbance at each specific concentration; the inset to Fig. 3(C) reveals the linear relationship used to calculate the LOD, through the 3σ method [LOD = 3 × (SD/S), where SD is the standard deviation and S is the slope of the plot]. The calculated LOD was 1160 copies/ml of target with a Pearson's *r* value of 0.99843, suggesting high sensitivity. Thus, our **PK-probe**/Lig-RPA system was extremely sensitive, functioning even in the presence of only small copy numbers of viral RNA from SARS-CoV-2. In general, RNA viruses have very low concentrations of their genomes; therefore, ultrasensitive detection is necessary. In our system, LOD was 1160 copies/ml, which is similar with RT-qPCR methods such as reported by Yang M, et al. and Corman et al. and even highly sensitive compared to other colorimetric detection method as we mentioned in Table S2 [33–37].

3.5. Selectivity

Theoretically, a general RT-RPA system cannot discriminate a perfectly matched sequence from one- or two-base-mismatched sequences, because when the reaction primers bind to the target RNA for the RT process, they might be able to amplify the gene with several mismatched-sequence amplicons (false positive). In contrast, we expected that our Lig-RPA system might discriminate mismatched points during the ligation step. It would form the full-length cDNA only when all of the ligation templates matched the viral RNA from SARS-CoV-2. SplintR ligase produces complementary cDNA sequences only in the presence of a matched target RNA sequence; if one of the ligation templates did not match, the cDNA would not be synthesized. Therefore, we expected that the selectivity of our Lig-RPA assay would be superior to that of general RT-RPA.

To determine the selectivity of our Lig-RPA detection method, we incorporated single, double, and triple mismatches in the ligation templates (LT3, tail region; LT4, head and mid region). To evaluate our **PK-probe**/Lig-RPA system's selectivity [Fig. 4(A) and (C), S2 and S3] we compared its selectivity to **PK-probe**/RT-RPA system's selectivity [Fig. 4(B) and (D) and S4]. For comparison of Lig-RPA and RT-RPA, we examined their amplified products using PAGE [Fig. 4(A) and (B)].

Fig. 4(A) and (B) display the results of PAGE-based comparisons of Lig-RPA and RT-RPA. The use of Lig-RPA with target RNA from SARS-CoV-2 revealed different gel band patterns in response to the different mismatched sequences, from one to three mismatches. In contrast, the RT-RPA assay revealed almost the same gel band patterns in response to the one to three mismatches, implying that the RT-RPA system could not discriminate false binding to similar sequences. In the colorimetric test performed using Lig-RPA, clearly differentiable color variations appeared among the various mismatched systems; in contrast, the RT-RPA–based colorimetric tests revealed almost the same color change in each case, leading to a high probability of false-positive outcomes [Fig. 4 (C) and (D)]. Thus, the PAGE and colorimetric tests indicated that the **PK-probe**/Lig-RPA system had higher selectivity for target-based detection.

To study the selectivity further, we employed several bacterial genomes to examine whether cross-reactions occurred when using **PK-probe**/Lig-RPA system. We prepared samples of nine species of bacteria that are known normal flora in the upper respiratory tract or frequent

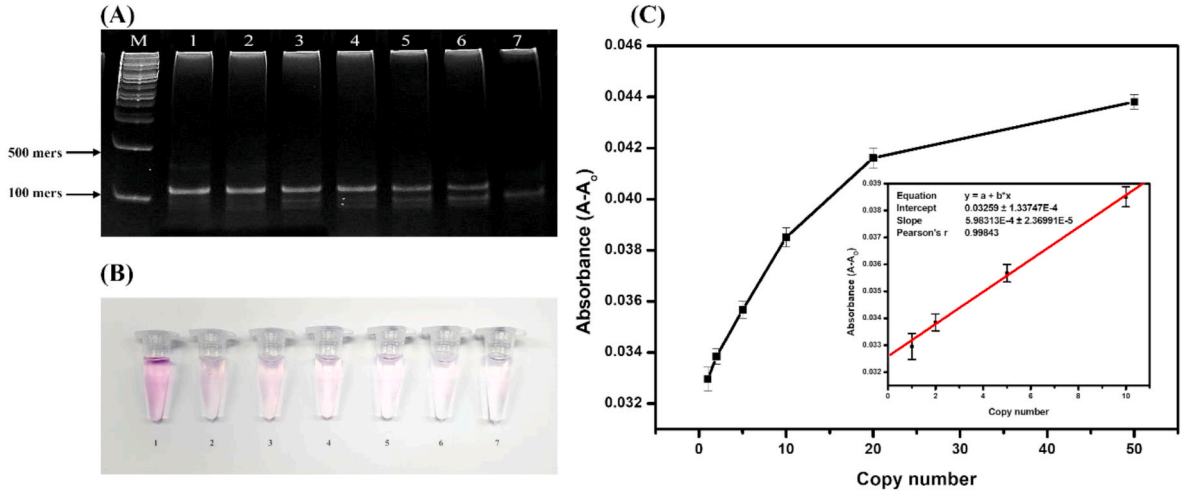

Fig. 3. Sensitivity of the reactions performed using the **PK-probe**/Lig-RPA assay. **(A)** PAGE analysis of the Lig-RPA sensitivity test with different copy numbers. Lane M: 100-bp ladder; lane 1: 50 copies; lane 2: 20 copies; lane 3: 10 copies; lane 4: 5 copies; lane 5: 2 copies; lane 6: 1 copy; lane 7: 0 copy. **(B)** Colorimetric analysis of the sensitivity test of Lig-RPA with **PK-probe** using different copy numbers. Lane 1: 0 copy; lane 2: 1 copy; lane 3: 2 copies; lane 4: 5 copies; lane 5: 10 copies; lane 6: 20 copies; lane 7: 50 copies. **(C)** Sensitivity study performed using full-genome SARS-CoV-2 at concentrations from 0 to 50 copies/reaction (copies/rxn). All reactions were repeated three times; error bars are presented in the graph. All absorbances were measured at 575 nm. *A*: Absorbance in the presence of target; A_0: absorbance in the absence of target; *y*-axis: absolute value. Obtained LOD was 1160 copies/ml (as target RNA used 1 μl), determined using the 3σ method [LOD = 3 × (SD/S), where SD is the standard deviation and S is the slope of the plot].

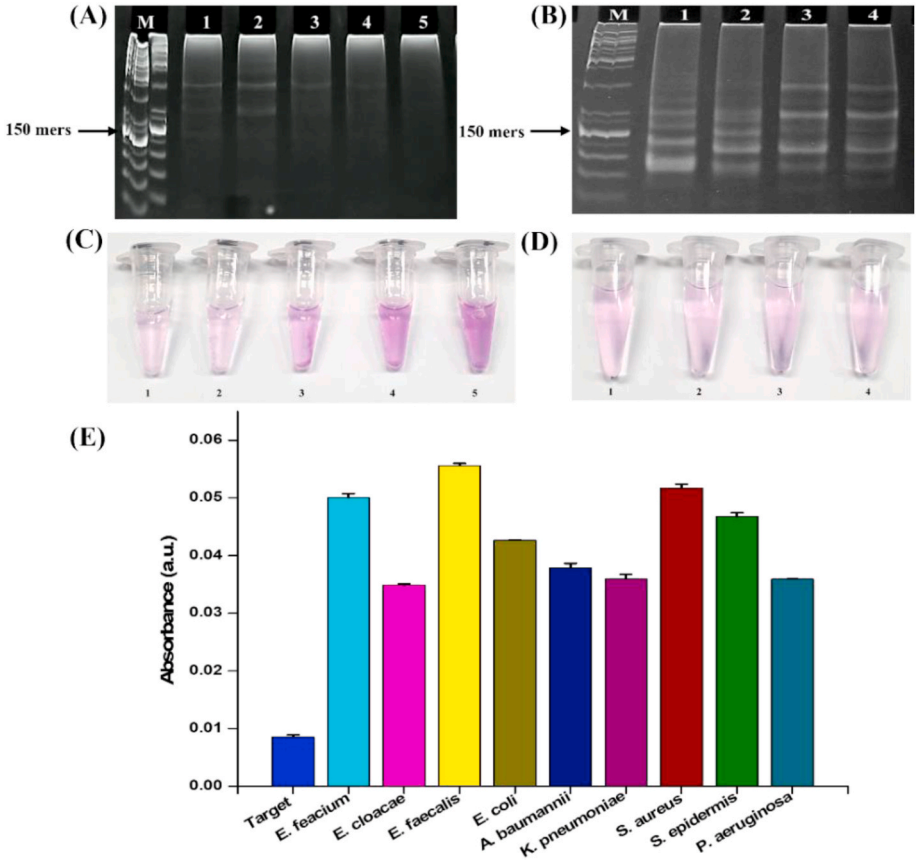

Fig. 4. (A) PAGE analysis of the **PK-probe**/Lig-RPA selectivity test. Lane M: 25/100-bp ladder; lane 1: **PK-probe**/Lig-RPA with middle 1 mismatch; lane 2: **PK-probe**/Lig-RPA; lane 3: **PK-probe**/Lig-RPA with 1 mismatch (head/ligation site); lane 4: **PK-probe**/Lig-RPA with 2 mismatches (head & middle); lane 5: **PK-probe**/Lig-RPA with 3 mismatches (head 1 & middle 2). **(B)** PAGE analysis of **PK-probe**/RT-RPA selectivity test with different mismatched reverse primers during cDNA synthesis. Lane M: 25/100-bp ladder; lane 1: **PK-probe**/RT-RPA positive; lane 2: **PK-probe**/RT-RPA with 1 mismatch; lane 3: **PK-probe**/RT-RPA with 2 mismatches; lane 4: **PK-probe**/RT-RPA with 3 mismatches. **(C)** Colorimetric analysis of the selectivity test of **PK-probe**/Lig-RPA Lane 1: **PK-probe**/Lig-RPA; lane 2: **PK-probe**/Lig-RPA with middle 1 mismatch; lane 3: **PK-probe**/Lig-RPA with 1 mismatch (head/ligation site); lane 4: **PK-probe**/Lig-RPA with 2 mismatches (head & middle); lane 5: **PK-probe**/Lig-RPA with 3 mismatches (head 1 & middle 2). **(D)** Colorimetric analysis of selectivity test of **PK-probe**/RT-RPA with different mismatched reverse primers during cDNA synthesis. Lane 1: **PK-probe**/RT-RPA positive; lane 2: **PK-probe**/RT-RPA with 1 mismatch; lane 3: **PK-probe**/RT-RPA with 2 mismatches; lane 4: **PK-probe**/RT-RPA with 3 mismatches. **(E)** Bar diagram of the selectivity of the **PK-probe**/Lig-RPA system operated in the presence of several bacterial genomes.

pathogens of respiratory tract infections (*S. aureus*, *S. epidermidis*, *E. faecalis*, *E. feacium*, *E. coli*, *K. pneumoniae*, *E. cloacae*, *P. aeruginosa*, and *A. baumannii*). We performed the **PK-probe**/Lig-RPA reactions with these nine types of bacterial genomes. Because COVID-19 samples are typically taken from the mouth and nose, the virus and some of these bacteria might be present if there were any bacterial infection. Any diagnostic system that reacted with these bacteria would diagnose the patient as a false positive; therefore, selective detection is imperative for practical application. These bacteria did not react with the **PK-probe**/Lig-RPA system; the absorbance values were almost negative because no amplification occurred and, therefore, the system could not produce PPi [Fig. 4(E) and S5,]. The colorimetric detection was consistent with the absorbance changes, as displayed in the bar diagram. Thus, based on this selectivity data, our **PK-probe**/Lig-RPA system displayed stronger selectivity than the **PK-probe**/RT-RPA system.

4. Validation with simulated sample of recombinant SARS-CoV-2

Our spiked SARS Cov-2 RNA included human genome RNA also; therefore, all our experiments featured this different background nucleic acid. One limitation of the study is that we had to rely on spiked-in materials and could not execute the performance of the assay using clinical SARS-CoV-2-positive samples; nevertheless, we developed an alternative approach to mimic real sample virus conditions. Here, we used the inactive recombinant SARS Cov-2 full genome material (fully extractable with a real viral protein coat) with nasopharyngeal sample using universal transport media (T-SWAB TRANSPORT Universal Transport Medium, Noble Biosciences, Hwaseong, Korea), which could be used for virus culturing, antigen testing, and PCR (by extraction). If any detection systems worked with this sample, then those systems would also function with real samples.

With our focus on POCT, we extracted RNA at 25 °C within 10 min by preparing the 6% formamide with 1X isothermal amplification buffer that had been described previously by Li et al. [38]. Although they had performed incubation at 65 °C, our recombinant SARS Cov-2 virus experiment demonstrated that, when using this extraction buffer, RNA extraction was possible at any temperature (25 °C, 37 °C, or 65 °C) and that our **PK-probe**/Lig-RPA system functioned well in simulated recombinant SARS Cov-2 virus experiments (Fig. S6). Accordingly, we believe that it would also function with real samples and for POCT.

5. Conclusion

We have developed a diagnostic system combining ligation-mediated recombinase polymerase isothermalamplification (Lig-RPA) and **PK-probe** (a PPi sensing colorimetric probe) for the detection of the target "Ngene" (nucleocapsid) of the SARS-CoV-2 genome. In a comparative study with other RT-based diagnosissystems (e.g., RT-RPA), our system displayed better selectivity toward SARS-CoV-2 in the presence of variousbacterial genomes, and it was simpler to perform with a very low chance of false-positive outcome. Furthermore, this **PK-probe**/Lig-RPA system has other attractive features for application in POCT: itsisothermal amplification occurs at room temperature, its diagnostic time is rapid (30 min), its sensitivity is high 1160 copies/ml, and its colorimetric detection by the naked eye is robust. Our developed system functions as a simple, affordable, and useful detection assay for SARS-CoV-2; we hope that it might also be useful for detecting other viruses and, thereby, be used in the diagnoses of various diseases.

Author contributions

Tasnima Alam Asa: Conceptualization, Methodology, Identification, Validation, Investigation, Formal analysis, Writing original draft,

Review & editing, Data curation, Visualization. Pradeep Kumar: Methodology, Synthesis, Identification, Visualization. Jaehyeon Lee: Validation, Visualization, spiked SARS-CoV-2 RNA sample and pseudo-virus experiment support. Young Jun Seo: Conceptualization, Resources, Formal analysis, Data curation, Writing review & editing, Supervision, Project administration, Funding acquisition.

Declaration of competing interest

The authors declare that they have no known competing financial interests or personal relationships that could have appeared to influence the work reported in this paper.

Data availability

The data that has been used is confidential.

Acknowledgment

This study was supported by the Basic Science Research Program through the National Research Foundation of Korea (2021R1A2C1003804), funded by the Republic of Korea.

Appendix A. Supplementary data

Supplementary data to this article can be found online at https://doi.org/10.1016/j.talanta.2022.123835.

References

[1] The Covid-19 pandemic - The New York Times (accessed March 7, 2022), https://www.nytimes.com/news-event/coronavirus.
[2] P. Ghosh, R. Chowdhury, M.E. Hossain, F. Hossain, M. Miah, M.U. Rashid, J. Baker, M.Z. Rahman, M. Rahman, X. Ma, M.S. Duthie, A.A. El Wahed, D. Mondal, Evaluation of recombinase-based isothermal amplification assays for point-of-need detection of SARS-CoV-2 in resource-limited settings, Int. J. Infect. Dis. 114 (2022) 105–111, https://doi.org/10.1016/j.ijid.2021.11.007.
[3] B. Wang, R. Li, Z. Lu, Y. Huang, Does comorbidity increase the risk of patients with covid-19: evidence from meta-analysis, Aging 12 (2020) 6049–6057, https://doi.org/10.18632/AGING.103000.
[4] R. Liu, H. Han, F. Liu, Z. Lv, K. Wu, Y. Liu, Y. Feng, C. Zhu, Positive rate of RT-PCR detection of SARS-CoV-2 infection in 4880 cases from one hospital in Wuhan, China, from Jan to Feb 2020, Clin. Chim. Acta 505 (2020) 172–175, https://doi.org/10.1016/j.cca.2020.03.009.
[5] I. Smyrlaki, M. Ekman, A. Lentini, N. Rufino de Sousa, N. Papanicolaou, M. Vondracek, J. Aarum, H. Safari, S. Muradrasoli, A.G. Rothfuchs, J. Albert, B. Högberg, B. Reinius, Massive and rapid COVID-19 testing is feasible by extraction-free SARS-CoV-2 RT-PCR, Nat. Commun. 11 (2020) 1–12, https://doi.org/10.1038/s41467-020-18611-5.
[6] C.P. Price, Regular review: point of care testing, Br. Med. J. 322 (2001) 1285–1288, https://doi.org/10.1136/bmj.322.7297.1285.
[7] Y. Sun, L. Yu, C. Liu, S. Ye, W. Chen, D. Li, W. Huang, One-tube SARS-CoV-2 detection platform based on RT-RPA and CRISPR/Cas12a, J. Transl. Med. 19 (2021) 1–10, https://doi.org/10.1186/s12967-021-02741-5.
[8] W. Feng, H. Peng, J. Xu, Y. Liu, K. Pabbaraju, G. Tipples, M.A. Joyce, H.A. Saffran, D.L. Tyrrell, S. Babiuk, H. Zhang, X.C. Le, Integrating reverse Transcription recombinase polymerase amplification with CRISPR technology for the one-tube Assay of RNA, Anal. Chem. 93 (2021) 12808–12816, https://doi.org/10.1021/acs.analchem.1c03456.
[9] D. Liu, H. Shen, Y. Zhang, D. Shen, M. Zhu, Y. Song, Z. Zhu, C. Yang, A microfluidic-integrated lateral flow recombinase polymerase amplification (MI-IF-RPA) assay for rapid COVID-19 detection, Lab Chip 21 (2021), https://doi.org/10.1039/D0LC01222J, 2019–2026.
[10] Z.A. Crannell, B. Rohrman, R. Richards-Kortum, Equipment-free incubation of recombinase polymerase amplification reactions using body heat, PLoS One 9 (2014) 1–7, https://doi.org/10.1371/journal.pone.0112146.
[11] R. Aman, A. Mahas, T. Marsic, N. Hassan, M.M. Mahfouz, Efficient, rapid, and sensitive detection of plant RNA viruses with one-Pot RT-RPA–CRISPR/Cas12a assay, Front. Microbiol. 11 (2020) 1–10, https://doi.org/10.3389/fmicb.2020.610872.
[12] D.K. Ghosh, S.B. Kokane, S. Gowda, Development of a reverse transcription recombinase polymerase based isothermal amplification coupled with lateral flow immunochromatographic assay (CTV-RT-RPA-LFICA) for rapid detection of Citrus tristeza virus, Sci. Rep. 10 (2020) 1–16, https://doi.org/10.1038/s41598-020-77692-w.
[13] C. Amaral, W. Antunes, E. Moe, A.G. Duarte, L.M.P. Lima, C. Santos, I.L. Gomes, G. S. Afonso, R. Vieira, H.S.S. Teles, M.S. Reis, M.A.R. da Silva, A.M. Henriques, M. Fevereiro, M.R. Ventura, M. Serrano, C. Pimentel, A molecular test based on RT-LAMP for rapid, sensitive and inexpensive colorimetric detection of SARS-CoV-2 in clinical samples, Sci. Rep. 11 (2021) 1–12, https://doi.org/10.1038/s41598-021-95799-6.
[14] Y. Li, L. Li, X. Fan, Y. Zou, Y. Zhang, Q. Wang, C. Sun, S. Pan, X. Wu, Z. Wang, Development of real-time reverse transcription recombinase polymerase amplification (RPA) for rapid detection of peste des petits ruminants virus in clinical samples and its comparison with real-time PCR test, Sci. Rep. 8 (2018) 1–9, https://doi.org/10.1038/s41598-018-35636-5.
[15] L. Lillis, D. Lehman, M.C. Singhal, J. Cantera, J. Singleton, P. Labarre, A. Toyama, O. Piepenburg, M. Parker, R. Wood, J. Overbaugh, D.S. Boyle, Non-instrumented incubation of a recombinase polymerase amplification assay for the rapid and sensitive detection of proviral hiv-1 dna, PLoS One 9 (2014), e108189, https://doi.org/10.1371/journal.pone.0108189.
[16] J. Jin, S. Vaud, A.M. Zhelkovsky, J. Posfai, L.A. McReynolds, Sensitive and specific miRNA detection method using SplintR Ligase, Nucleic Acids Res. 44 (2016) e116, https://doi.org/10.1093/nar/gkw399.
[17] P. Craw, W. Balachandran, Isothermal nucleic acid amplification technologies for point-of-care diagnostics: a critical review, Lab Chip 12 (2012) 2469–2486, https://doi.org/10.1039/c2lc40100b.
[18] SARS-CoV-2 Resources - NCBI (accessed March 3, 2022), https://www.ncbi.nlm.nih.gov/sars-cov-2/.
[19] J. Qian, S.A. Boswell, C. Chidley, Z. xiang Lu, M.E. Pettit, B.L. Gaudio, J. M. Fajnzylber, R.T. Ingram, R.H. Ward, J.Z. Li, M. Springer, An enhanced isothermal amplification assay for viral detection, Nat. Commun. 11 (2020) 1–10, https://doi.org/10.1038/s41467-020-19258-y.
[20] M. Shin, P. Meda Krishnamurthy, G. Devi, J.K. Watts, Quantification of antisense oligonucleotides by splint ligation and quantitative polymerase chain reaction, Nucleic Acid Therapeut. 32 (2022) 66–73, https://doi.org/10.1089/nat.2021.0040.
[21] Y. Geng, K. Tan, L. Liu, X.X. Sun, B. Zhao, J. Wang, Development and evaluation of a rapid and sensitive RPA assay for specific detection of Vibrio parahaemolyticus in seafood, BMC Microbiol. 19 (2019) 186, https://doi.org/10.1186/s12866-019-1562-z.
[22] C.C. Conrad, R.K. Daher, K. Stanford, K.K. Amoako, M. Boissinot, M.G. Bergeron, T. Alexander, S. Cook, B. Ralston, R. Zaheer, Y.D. Niu, T. McAllister, A sensitive and accurate recombinase polymerase amplification assay for detection of the primary bacterial pathogens causing bovine respiratory disease, Front. Vet. Sci. 7 (2020) 208, https://doi.org/10.3389/fvets.2020.00208.
[23] H.N. Wilson, Absorptiometry and "colorimetric analysis, in: An Approach to Chem. Anal., Pergamon, 1966, pp. 222–259, https://doi.org/10.1016/b978-0-08-011543-6.50016-3.
[24] C. Dong, X. Ma, N. Qiu, Y. Zhang, A. Wu, An ultra-sensitive colorimetric sensor based on smartphone for pyrophosphate determination, Sens. Actuators B Chem. 329 (2021), 129066, https://doi.org/10.1016/j.snb.2020.129066.
[25] C.Y. Chen, Y.Z. Tan, P.H. Hsieh, C.M. Wang, H. Shibata, K. Maejima, T.Y. Wang, Y. Hiruta, D. Citterio, W.S. Liao, Metal-free colorimetric detection of pyrophosphate ions by inhibitive nanozymatic carbon dots, ACS Sens. 5 (2020) 1314–1324, https://doi.org/10.1021/acssensors.9b02486.
[26] P. Kumar, G.S.R. Kumara, Y.J. Seo, Copper complex of a thienyl-hydrazone rhodamine derivative is a highly selective colorimetric sensor for pyrophosphate, Tetrahedron Lett. 89 (2022), 153606, https://doi.org/10.1016/j.tetlet.2021.153606.
[27] A. Lázaro, E.S. Yamanaka, Á. Maquieira, L.A. Tortajada-Genaro, Allele-specific ligation and recombinase polymerase amplification for the detection of single nucleotide polymorphisms, Sens. Actuators B Chem. 298 (2019), 126877, https://doi.org/10.1016/j.snb.2019.126877.
[28] A. Pandith, Y.J. Seo, Label-free sensing platform for miRNA-146a based on chromo-fluorogenic pyrophosphate recognition, J. Inorg. Biochem. 203 (2020), 110867, https://doi.org/10.1016/j.jinorgbio.2019.110867.
[29] M.H. Choi, Y.J. Seo, Rapid and highly sensitive hairpin structure-mediated colorimetric detection of miRNA, Anal. Chim. Acta 1176 (2021), 338765, https://doi.org/10.1016/j.aca.2021.338765.
[30] Y. Shi, J. Wang, K. Mu, S. Liu, G. Yang, M. Zhang, J. Yang, Copper (Ii) ion-modified gold nanoclusters as peroxidase mimetics for the colorimetric detection of pyrophosphate, Sensors 21 (2021) 5538, https://doi.org/10.3390/s21165538.
[31] I.M. Lobato, C.K. O'Sullivan, Recombinase polymerase amplification: basics, applications and recent advances, TrAC, Trends Anal. Chem. 98 (2018) 19–35, https://doi.org/10.1016/j.trac.2017.10.015.
[32] R.K. Daher, G. Stewart, M. Boissinot, M.G. Bergeron, Recombinase polymerase amplification for diagnostic applications, Clin. Chem. 62 (2016) 947–958, https://doi.org/10.1373/clinchem.2015.245829.
[33] M. Yang, S. Cao, Y. Liu, Z. Zhang, R. Zheng, Y. Li, J. Zhou, C. Zong, D. Cao, X. Qin, Performance verification of five commercial RT-qPCR diagnostic kits for SARS-CoV-2, Clin. Chim. Acta 525 (2022) 46–53, https://doi.org/10.1016/j.cca.2021.12.004.
[34] V.M. Corman, O. Landt, M. Kaiser, R. Molenkamp, A. Meijer, D.K.W. Chu, T. Bleicker, S. Brünink, J. Schneider, M.L. Schmidt, D.G.J.C. Mulders, B. L. Haagmans, B. Van Der Veer, S. Van Den Brink, L. Wijsman, G. Goderski, J. L. Romette, J. Ellis, M. Zambon, M. Peiris, H. Goossens, C. Reusken, M.P. G. Koopmans, C. Drosten, Detection of 2019 novel coronavirus (2019-nCoV) by real-time RT-PCR, Euro Surveill. 25 (2020) 1, https://doi.org/10.2807/1560-7917.ES.2020.25.3.2000045.
[35] M.H. Choi, J. Lee, Y.J. Seo, Dual-site ligation-assisted loop-mediated isothermal amplification (dLig-LAMP) for colorimetric and point-of-care determination of real

SARS-CoV-2, Microchim. Acta 189 (2022), https://doi.org/10.1007/s00604-022-05293-7, 1–10.
[36] M.N. Aoki, B. de Oliveira Coelho, L.G.B. Góes, P. Minoprio, E.L. Durigon, L. G. Morello, F.K. Marchini, I.N. Riediger, M. do Carmo Debur, H.I. Nakaya, L. Blanes, Colorimetric RT-LAMP SARS-CoV-2 diagnostic sensitivity relies on color interpretation and viral load, Sci. Rep. 11 (2021) 1–10, https://doi.org/10.1038/s41598-021-88506-y.
[37] C. Rodríguez Díaz, N. Lafuente-Gómez, C. Coutinho, D. Pardo, H. Alarcón-Iniesta, M. López-Valls, R. Coloma, P. Milán-Rois, M. Domenech, M. Abreu, R. Cantón, J. C. Galán, R. Bocanegra, L.A. Campos, R. Miranda, M. Castellanos, Á. Somoza, Development of colorimetric sensors based on gold nanoparticles for SARS-CoV-2 RdRp, E and S genes detection, Talanta 243 (2022), 123393, https://doi.org/10.1016/j.talanta.2022.123393.
[38] J. Li, X. Hu, X. Wang, J. Yang, L. Zhang, Q. Deng, X. Zhang, Z. Wang, T. Hou, S. Li, A novel One-pot rapid diagnostic technology for COVID-19, Anal. Chim. Acta (2021) 1154, https://doi.org/10.1016/j.aca.2021.338310.